



## Computational investigation of the isomers formed from the reaction $S_2 + O_2$

Nadia Sebbar, Henning Bockhorn, Joseph W. Bozzelli & Dimosthenis Trimis

To cite this article: Nadia Sebbar, Henning Bockhorn, Joseph W. Bozzelli & Dimosthenis Trimis (05 Mar 2025): Computational investigation of the isomers formed from the reaction  $S_2 + O_2$ , Journal of Sulfur Chemistry, DOI: [10.1080/17415993.2025.2473740](https://doi.org/10.1080/17415993.2025.2473740)

To link to this article: <https://doi.org/10.1080/17415993.2025.2473740>



© 2025 Karlsruher Institut für Technologie (KIT). Published by Informa UK Limited, trading as Taylor & Francis Group



View supplementary material [↗](#)



Published online: 05 Mar 2025.



Submit your article to this journal [↗](#)



Article views: 104



View related articles [↗](#)



View Crossmark data [↗](#)

# Computational investigation of the isomers formed from the reaction $S_2 + O_2$

Nadia Sebbar<sup>a</sup>, Henning Bockhorn<sup>a</sup>, Joseph W. Bozzelli<sup>b</sup> and Dimosthenis Trimis<sup>a</sup>

<sup>a</sup>Engler-Bunte Institut/Verbrennungstechnik, Karlsruher Institut für Technologie, Karlsruhe, Germany;

<sup>b</sup>Department of Chemical Engineering, New Jersey Institute of Technology, Newark, NJ, United States

## ABSTRACT

The reaction of disulfur ( $^3S_2$ ) with oxygen  $^3S_2 + ^3O_2$  is an important reaction in sulfur combustion leading to different  $^1S_2O_2$  isomers and subsequent intramolecular isomerization reactions. In this work reaction paths and products resulting from the reaction  $^3S_2 + ^3O_2$  are investigated computationally using four different quantum chemistry methods. The thermochemistry of the isomerization and dissociation reactions for species involved in this system is evaluated in detail and reported along with reaction paths and energy barriers. Enthalpies are calculated on CBS-QB3, G3B3, G4 levels of calculation and, whenever possible, on W1U levels. Entropy and heat capacity contributions versus temperature are determined from molecular structures, moments of inertia and vibrational frequencies. Importance of the reaction paths and kinetic parameters using bimolecular chemical activation analysis are estimated as function of temperature from the calculated thermochemical data. High pressure limit kinetic parameters are obtained from canonical transition state theory (TST) calculations. Results show that  $^1SS(=O)=O$ ,  $^3SO$ ,  $^1SO_2$  and  $^3S$  are the low energy products.<sup>1</sup>

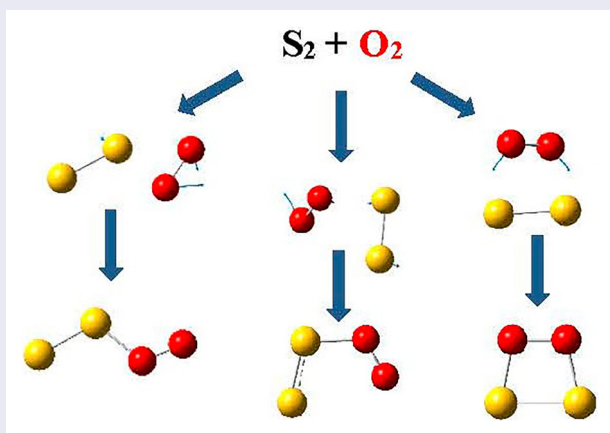
## ARTICLE HISTORY

Received 23 September 2024


Accepted 24 February 2025

## KEYWORDS

Sulfur combustion; oxidation; thermochemistry;  $S_2O_2$



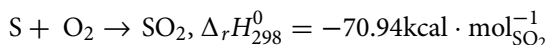
**CONTACT** Nadia Sebbar  nadia.sebbar@partner.kit.edu  Engler-Bunte Institut/Verbrennungstechnik, Karlsruher Institut für Technologie, Engler-Bunte-Ring 7, Karlsruhe 76131, Germany

 Supplemental data for this article can be accessed online at <https://doi.org/10.1080/17415993.2025.2473740>.

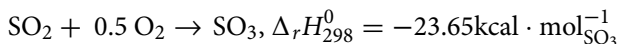
© 2025 Karlsruher Institut für Technologie (KIT). Published by Informa UK Limited, trading as Taylor & Francis Group  
This is an Open Access article distributed under the terms of the Creative Commons Attribution License (<http://creativecommons.org/licenses/by/4.0/>), which permits unrestricted use, distribution, and reproduction in any medium, provided the original work is properly cited. The terms on which this article has been published allow the posting of the Accepted Manuscript in a repository by the author(s) or with their consent.

## 1. Introduction

Sulfur is an energy carrier which can be easily handled and stored and, therefore, has gained in interest for closed energy conversion cycles. The conception of such energy cycles is to use the heat released from combustion of sulfur to generate electricity and to recover elemental sulfur from the combustion products by providing and integrating energy from *e.g.* renewable sources [1]. Processes of this kind benefit from the comparatively low costs of sulfur which can be inexpensively stored outdoor under ambient conditions and for long times as well as in large quantities [2,3]. Furthermore, combustion of elemental sulfur can be performed on large-scale as part of the industrial production of sulfuric acid, which is one of the world's largest-volume industrial chemicals. Most of the existing sulfur combustion facilities are technically robust and designed to realize large product streams. Within the projects PEGASUS (Renewable Power Generation by Solar Particle Receiver Driven Sulfur Storage Cycle [2]) and SULPHURREAL (An innovative thermochemical cycle based on solid sulfur for integrated long-term storage of solar thermal [3]) a novel power cycle for electricity production from renewable sources applying a particle receiver for solar energy combined with a sulfur storage system and a sulfuric acid production system is investigated. The process is based on solid particles as heat transfer medium enabling storage of solar energy as thermal energy and also as chemical energy in solid sulfur, rendering thus a solar power plant capable of round-the-clock electricity production from renewable sources. The main chemical reaction steps to be integrated into the sulfuric acid production are first the combustion of sulfur:

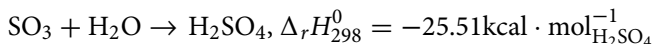


and the subsequent catalytic conversion to  $\text{SO}_3$ :

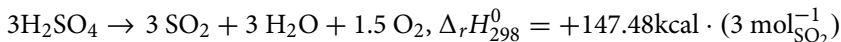


The energy released in the combustion of sulfur is utilized by a combined cycle (gas & steam turbine) to generate electricity.

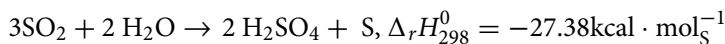
Sulfuric acid produced from  $\text{SO}_3$  via:



is thermally decomposed at temperatures above 800 °C into  $\text{SO}_2$ ,  $\text{O}_2$  and  $\text{H}_2\text{O}$ :



followed by the disproportionation of  $\text{SO}_2$  at temperatures below 200 °C.



The heat of reaction for the endothermic decomposition of  $\text{H}_2\text{SO}_4$  is provided from solar energy. The overall process can be shifted from pure sulfuric acid production to partially/complete recycling of sulfur via decomposition of sulfuric acid in the closed energy conversion cycle depending on the demand of sulfuric acid and the availability of solar energy. A more detailed description of the conception of the closed energy conversion process is given in [4].

For the design and optimization of combustion devices for sulfur providing high power densities the knowledge of validated reaction mechanisms are prerequisites. Since research on combustion of sulfur is motivated primarily by the frequently applied Claus-process, most reaction mechanisms from literature describe the reactions of sulfur compounds in combination with hydrocarbon or hydrogen combustion. However, only few of them consider the oxidation of sulfur in the absence of hydrogen or hydrocarbons. The scope of this study is, therefore, to develop and evaluate rate coefficients of reactions involving oxygenated sulfur excluding hydrocarbons and hydrogen.

The reaction  $^3\text{S}_2 + ^3\text{O}_2 \rightarrow ^1\text{S}_2\text{O}_2$ , constituting an important reaction in sulfur combustion, is a complex reaction leading to several intermediates and isomers through different intramolecular reactions. One of the first theoretical studies to identify the different isomers resulting from this reaction system has been performed by Marsden and Smith [5]. They reported the occurrence of different possible isomers of  $\text{S}_2\text{O}_2$ , in both singlet and triplet states. Their calculations resulted in thirteen singlet and six triplet  $\text{S}_2\text{O}_2$  isomers, the lowest energy isomer being a singlet. In their ab initio methods, a DZ(P) basis was used for most calculations and a larger TZ(2)P basis was used for a few selected calculations. All geometries were fully optimized and the nine most stable singlet isomers were found to be true local minima on the SCF level of calculations.

Reaction rates for the reaction  $\text{S} + \text{SO}_2 \rightarrow 2 \text{SO}$  have been investigated experimentally by Murakami *et al.* [6] over the temperature range between 1120 and 2800 K. They measured the time evolution of S atoms behind reflected shock waves. The experiments resulted in a non-Arrhenius temperature dependence of the rate coefficient. The rate coefficients derived from a conventional transition-state theory calculated on the G2M-(CC1) level could not explain the experimental observations, however, the authors suggest that the reaction proceeds only on the triplet surfaces via the intermediate  $\text{S}_2\text{O}_2$  complex.

Ramírez-Solís *et al.* [7] performed Born–Oppenheimer DFT molecular dynamics (BO-DFT-MD) simulations for the three lowest energy isomers of  $\text{S}_2\text{O}_2$  using the B3PW91/aug-cc-pVTZ method. Three isomers of  $\text{S}_2\text{O}_2$  were investigated at room temperature: the trigonal  $\text{SS}(=\text{O})=\text{O}$ , the cyclic  $\text{O}=\text{Y}(\text{SOS})$  and the *cis*-OSSO.

Two studies report electronic transitions in molecules that may exist in the atmosphere of the Venus [8,9]. Two different  $\text{S}_2\text{O}_2$  isomers, *cis*-OSSO and *trans*-OSSO were identified as important sulfur reservoirs in the atmosphere of the Venus. Based on observations of SO [10] and the measured rate coefficient for its self-reaction, they estimated the formation rate of the two isomers. The rate coefficient of OSSO formation in the low-pressure limit was measured to be  $k_0 = 4.4 \times 10^{-31} \text{ molecule}^{-2} \cdot \text{cm}^6 \cdot \text{s}^{-1}$  at  $T = 298 \text{ K}$  and  $p = 2\text{--}8 \text{ Torr}$  of  $\text{N}_2$  with an estimated  $\pm 50\%$  uncertainty. The barrierless OSSO formation allowed the authors to estimate a high-pressure limit rate constant with collision theory to  $k_\infty = 1.4 \times 10^{-11} \text{ molecule}^{-1} \cdot \text{cm}^3 \cdot \text{s}^{-1}$  at  $T = 245 \text{ K}$ .

In a recent study Hochlaf *et al.* [11] performed accurate ab initio calculations to investigate the electronic structure, relative stability, and spectra of the stable isomers of the  $\text{S}_2\text{O}_2$  system. Special focus was on the most relevant isomers that could be involved in terrestrial and planetary atmospheres. The study reports several stable isomers for which geometric parameters, fragmentation energies, and simple and double ionization energies of the neutral species were calculated.

Abumounshar *et al.* [12] report and validate a detailed reaction mechanism for the oxidation of sulfur using experimental data from lab-scale reactors and a sulfur furnace from

a sulfuric acid plant. The developed model was used to investigate the effect of varying the relative air flow rates and oxygen enrichment on the exhaust gas temperature and the concentrations of  $\text{SO}_2$ ,  $\text{SO}_3$ , and  $\text{O}_2$  in the furnace. Dominant reaction pathways for the production of  $\text{SO}_2$  and  $\text{SO}_3$ , are identified. They report that the air/sulfur ratio monitors the furnace temperature and can be used to obtain the desired  $\text{O}_2/\text{SO}_2$  ratio at the furnace exit for the optimal operation of the subsequent catalytic converter for  $\text{SO}_2$  oxidation to  $\text{SO}_3$  in the sulfuric acid plant.

Goodarzi *et al.* [13] investigated the reaction pathways of  $\text{S} + \text{SO}_2$  on the G3B3//B3LYP/6-311++G(3df,3pd) level considering both triplet and singlet potential energy surfaces. Their main objective was to understand the reaction mechanism to explain the formation and decomposition of *trans*- $^1\text{OSSO}$  and *cis*- $^1\text{OSSO}$  complexes and to provide further information about gas phase reaction of  $\text{S} + ^1\text{SO}_2$  on the triplet and singlet potential energy surfaces. Their calculated results show four sets of products  $^3\text{SO} + ^3\text{SO}$ , *trans*- $^1\text{OSSO}$ , *cis*- $^1\text{OSSO}$  and  $^3\text{S}_2 + ^3\text{O}_2$ . In a following work Goodarzi *et al.* [14] investigated the reverse reaction pathway of  $\text{S}_2$  with oxygen on the triplet and singlet potential energy surface on the G3B3//B3LYP/6-311++G(3df,3pd) level calculation.

In this study we investigate the reaction  $^3\text{S}_2 + ^3\text{O}_2$  on high computational level and compare the formation of the intermediate compounds along with the enthalpies with the above mentioned studies. We also compare the identified reaction channels with those reported in [13,14], which however show several discrepancies but conduct to the same products. Kinetic calculations are subsequently performed to estimate rate coefficients of the different reaction paths.

## 2. Computational methods

Thermodynamic and kinetic properties of compounds resulting from the reaction  $^3\text{S}_2 + ^3\text{O}_2$  are estimated with the help of computational methods contained in the Gaussian 03 and Gaussian 09 program suite [15]. Based on previous studies [16,17] the calculations have been conducted using four ab-initio methods: CBS-QB3 [18], G3B3 (G3//B3LYP) [19,20], G4 [21] and W1 [22]. With CBS-QB3 and G3B3, structures and zero point vibrational energies are calculated on the B3LYP level.

The Gaussian-4 (G4) theory succeeded the G3 theory and among the improvements the QCISD(T) method is replaced by the CCSD(T) method for the highest level of correlation treatment. In addition, two new higher level corrections are added to try and account for deficiencies in the energy calculations. The W1 (Weizmann-1) theory, which calculates energies of compounds containing first-and second-row elements with very high accuracy, is applied in this study for a number of species.

## 3. Results

### 3.1. Enthalpies of formation

Standard enthalpies of formation for compounds resulting from the  $^3\text{S}_2 + ^3\text{O}_2$  reaction as well as their structures are reported in Table 2. For the calculation of standard enthalpies of formation, working reactions are employed, see Table 2. Standard enthalpies of formation

**Table 1.** Heat of reaction  $\Delta_r H_{298}^0$  for  ${}^3\text{S}_2 + {}^3\text{O}_2$  to  $2 {}^3\text{SO}$  and  ${}^3\text{S} + {}^1\text{SO}_2$  calculated on CBS-QB3, G3B3, G4 and W1U levels and compared with literature.

${}^3\text{S}_2 + {}^3\text{O}_2 \rightarrow 2 {}^3\text{SO}$			${}^3\text{S}_2 + {}^3\text{O}_2 \rightarrow {}^3\text{S} + {}^1\text{SO}_2$		
$\Delta_r H_{298}^0$	HF	kcal·mol <sup>-1</sup>	$\Delta_r H_{298}^0$	HF	kcal·mol <sup>-1</sup>
Literature		<b>−28.336</b>	Literature		<b>−35.430</b>
CBS-QB3	−0.044739	−27.074	CBS-QB3	−0.0529	−33.206
G3	−0.046659	−29.279	G3	−0.0537	−33.752
G3B3	−0.045837	−28.763	G3B3	−0.05423	−34.033
G4	−0.045491	<b>−28.546</b>	G4	−0.05579	<b>−35.008</b>
W1U	−0.043526	−27.313	W1U	−0.05449	−34.195

for  ${}^3\text{S}$ ,  ${}^3\text{S}_2$  [23],  ${}^3\text{SO}$  and  ${}^1\text{SO}_2$ ,  ${}^1\text{SSO}$  [24] used as reference in the work reactions are taken from the literature.

To check the reliability and accuracy of the methodology, the heat of reaction  $\Delta_r H_{298}^0$  was calculated for the reaction  ${}^3\text{S}_2 + {}^3\text{O}_2 \rightarrow 2 {}^3\text{SO}$  and  ${}^3\text{S}_2 + {}^3\text{O}_2 \rightarrow {}^3\text{S} + {}^1\text{SO}_2$  using the literature values of  ${}^3\text{S}_2$ ,  ${}^3\text{O}_2$ ,  ${}^3\text{SO}$  and  ${}^1\text{SO}_2$  and listed in Table 1 (in HF-units and kcal·mol<sup>-1</sup>). The values are compared with the results obtained with CBS-QB3, G3B3, G4 and W1U. As it can be seen in Table 1, there is a good agreement among literature data and the present calculations. We note in both cases that the best agreement is obtained with G4.

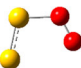
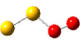
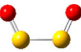
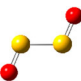
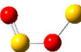
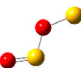


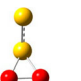
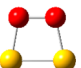
There is relatively little data on oxygenated sulfur compounds available in the literature for reaction systems without hydrocarbons. As far as the authors are aware, none of the literature studies on these species report W1U calculations preventing a comparison. Moreover, there is no study showing that W1U is the most accurate in the case of sulfur compounds.

In this study, the recommended values for the calculated enthalpy of formation are for most investigated species those obtained with G4 calculations. This is based on the fact that.

- (i) not all methods could find an optimal geometry or transition state (TST)
- (ii) W1U couldn't find all transition state structures
- (iii) several W1U results are somehow higher than those from the other methods and different from available literature values.
- (iv) Whatever the method, if a calculated enthalpy deviates significantly from the others, the geometry is checked carefully.

Calculated enthalpies of formation listed in Table 2 are compared with available literature values. Overall, the results show good precision among the four applied methods. The reaction of  ${}^3\text{S}_2$  with  ${}^3\text{O}_2$  leads to three different initial geometric structures (isomers) resulting from the association paths. Further isomerization results in several additional structures. The different structures are illustrated in Table 2. Two compounds result from the direct addition of an O atom to an S atom forming two different  ${}^1\text{SSOO}$  isomers in *cis* and *trans* configuration. The *cis*- ${}^1\text{SSOO}$  isomer is calculated to be more stable than the *trans* one, lower in energy by nearly 10 kcal·mol<sup>-1</sup>. The enthalpies for *cis*- ${}^1\text{SSOO}$  and *trans*- ${}^1\text{SSOO}$  calculated with the G4 method amount to 29.03 kcal mol<sup>-1</sup> and 38.01 kcal·mol<sup>-1</sup>,

**Table 2.** Standard enthalpy of formation  $\Delta_f H_{298}^0$  for singlet species in the  $^3S_2 + ^3O_2$  system calculated on CBS-QB3, G3B3, G4 and W1U levels (when possible) in kcal mol $^{-1}$ , Y means cyclic.

Structure	Working reactions used for $\Delta_f H_{298}^0$ calculation	$\Delta_f H_{298}^0$ in kcal·mol <sup>-1</sup>				Lit.
		CBS-QB3	G3B3	G4	W1U	
Reference data: <sup>3</sup> S: 66.24; <sup>3</sup> S <sub>2</sub> : 30.74; <sup>3</sup> SO: 1.2; <sup>1</sup> SO <sub>2</sub> : -70.94; <sup>1</sup> SSO: -13.5; <sup>3</sup> O: 58						
	<sup>3</sup> S <sub>2</sub> + <sup>3</sup> O <sub>2</sub> → <i>cis</i> - <sup>1</sup> SSOO	31.56	28.57	29.73	34.68	27.62 [13]
	2 <sup>3</sup> SO → <i>cis</i> - <sup>1</sup> SSOO	30.10	29.00	29.94	33.66	
	<i>cis</i> - <sup>1</sup> SSOO → <sup>3</sup> SSO + <sup>3</sup> O	27.53	24.98	28.69	31.52	
	<i>cis</i> - <sup>1</sup> SSOO → <sup>1</sup> SO <sub>2</sub> + <sup>3</sup> S	29.34	27.18	29.31	33.45	
	Average	29.93	27.43	<b>29.03</b>	33.33	
	<sup>3</sup> S <sub>2</sub> + <sup>3</sup> O <sub>2</sub> → <i>trans</i> - <sup>1</sup> SSOO	42.72	37.75	38.71	41.70	37.06 [13]
	2 <sup>3</sup> SO → <i>trans</i> - <sup>1</sup> SSOO	42.46	38.18	38.92	40.68	
	<i>trans</i> - <sup>1</sup> SSOO → <sup>1</sup> SSO + <sup>3</sup> O	38.69	34.16	36.12	38.54	
	<i>trans</i> - <sup>1</sup> SSOO → <sup>1</sup> SO <sub>2</sub> + <sup>3</sup> S	40.49	36.36	38.29	40.47	
	Average	41.09	36.61	<b>38.01</b>	40.35	
	<sup>3</sup> S <sub>2</sub> + <sup>3</sup> O <sub>2</sub> → <i>cis</i> - <sup>1</sup> OSSO	-29.26	-28.26	-29.61	-30.95	-29.23 [13]
	2 <sup>3</sup> SO → <i>cis</i> - <sup>1</sup> OSSO	-29.53	-27.83	-30.40	-31.97	
	<i>cis</i> - <sup>1</sup> OSSO → <sup>1</sup> SO <sub>2</sub> + <sup>3</sup> S	-31.49	-29.65	-30.03	-32.19	
	Average	-30.09	-28.58	<b>-29.68</b>	-31.70	
	<sup>3</sup> S <sub>2</sub> + <sup>3</sup> O <sub>2</sub> → <i>trans</i> - <sup>1</sup> OSSO	-26.46	-25.23	-26.51	-27.75	-26.22 [13]
	2 <sup>3</sup> SO → <i>trans</i> - <sup>1</sup> OSSO	-27.92	-24.80	-26.30	-28.77	
	<i>trans</i> - <sup>1</sup> OSSO → <sup>1</sup> SO <sub>2</sub> + <sup>3</sup> S	-28.68	-26.62	-26.93	-28.98	
	Average	-27.37	-25.55	<b>-26.58</b>	-28.50	
	<sup>3</sup> S <sub>2</sub> + <sup>3</sup> O <sub>2</sub> → <i>cis</i> - <sup>1</sup> SOSO	-7.76	-8.90	-9.92	-7.01	-9.72 [13]
	2 <sup>3</sup> SO → <i>cis</i> - <sup>1</sup> SOSO	-9.22	-8.48	-9.71	-8.03	
	<i>cis</i> - <sup>1</sup> SOSO → <sup>1</sup> SO <sub>2</sub> + <sup>3</sup> S	-9.98	-10.30	-10.34	-8.24	
	Average	-8.59	-9.23	<b>-9.99</b>	-7.76	
	<sup>3</sup> S <sub>2</sub> + <sup>3</sup> O <sub>2</sub> → <i>trans</i> - <sup>1</sup> SOSO	-0.77	-2.47	-2.76	-0.38	-2.44 [13]
	2 <sup>3</sup> SO → <i>trans</i> - <sup>1</sup> SOSO	-2.23	-2.04	-2.55	-1.41	
	<i>trans</i> - <sup>1</sup> SOSO → <sup>1</sup> SO <sub>2</sub> + <sup>3</sup> S	-2.99	-3.87	-3.19	-1.62	
	Average	-1.18	-2.79	<b>-2.84</b>	-1.14	
	<sup>1</sup> SO <sub>2</sub> + <sup>3</sup> S → <sup>1</sup> SS(=O)=O	-42.39	-40.10	-41.61	-42.27	-39.34 [13]
	<sup>1</sup> SSO + <sup>3</sup> O → <sup>1</sup> SS(=O)=O	-44.19	-42.29	-43.78	-44.20	
	Average	-43.29	-41.20	<b>-42.69</b>	-43.24	
	<sup>1</sup> SO <sub>2</sub> + <sup>3</sup> S → <sup>1</sup> Y(SSO)=O	-24.08	-22.54	-24.18	-24.47	-21.89 [13]
	<sup>1</sup> SSO + <sup>3</sup> O → <sup>1</sup> Y(SSO)=O	-25.88	-24.74	-26.35	-26.40	
	Average	-24.98	-23.64	<b>-25.27</b>	-25.44	
	<sup>1</sup> SO <sub>2</sub> + <sup>3</sup> S → <sup>1</sup> Y(SOO)=S	25.82	27.51	25.98	25.99	G3 26.32
	<sup>1</sup> SSO + <sup>3</sup> O → <sup>1</sup> Y(SOO)=S	24.01	25.32	23.80	24.06	
	Average	24.92	26.42	<b>24.89</b>	25.02	
	<sup>3</sup> S <sub>2</sub> + <sup>3</sup> O <sub>2</sub> → <sup>1</sup> Y(SSOO)	57.08	57.92	55.42	57.08	G3 26.32
	2 <sup>3</sup> SO → <sup>1</sup> Y(SSOO)	56.82	58.35	55.63	56.06	
	<sup>1</sup> Y(SSOO) + <sup>3</sup> SO → <sup>1</sup> SO <sub>2</sub> + <sup>1</sup> SSO	53.52	53.51	53.26	55.26	
	<sup>1</sup> Y(SSOO) → <sup>1</sup> SSO + <sup>3</sup> O	53.05	54.33	52.82	53.92	
	Average	55.12	56.03	<b>54.28</b>	55.58	

respectively. We note the excellent agreement of our calculated G3B3 value with the G3B3 values of Goodarzi *et al.* [13].

Further reactions/isomerizations of the *cis*- and *trans*- $^1SSOO$  isomers formed from the reaction  $^3S_2 + ^3O_2$  lead to *cis*- $^1OSSO$  and *trans*- $^1OSSO$  at approximately the same energy



of  $-29.68 \text{ kcal}\cdot\text{mol}^{-1}$  and  $-26.58 \text{ kcal}\cdot\text{mol}^{-1}$ , respectively. Data on these two isomers including standard enthalpies from refs. [8,13] were also reported in refs. [5–7]. Literature values are listed in Tables 2 and 3 for comparison with the present calculations. Table 2 shows that the calculated G3B3 and G4 values are in good agreement with the values reported in reference [13] for the *cis*- $^1\text{OSSO}$  and *trans*- $^1\text{OSSO}$  isomers. We note a deviation of  $5 \text{ kcal}\cdot\text{mol}^{-1}$  from the data in ref. [8]. It is important to point out that no experimental data is available to validate the accuracy of the values.

A different set of isomers, *cis*- $^1\text{SOSO}$  and *trans*- $^1\text{SOSO}$  are formed at higher energy of  $-10.0 \text{ kcal}\cdot\text{mol}^{-1}$  and  $-2.84 \text{ kcal}\cdot\text{mol}^{-1}$ , respectively. These values are in good agreement with values of ref. [13]. Formation of a cyclic compound  $^1\text{Y}(\text{SSO}) = \text{O}$  occurs at a relatively low energy of  $-25.27 \text{ kcal}\cdot\text{mol}^{-1}$  despite its strained 3-membered ring. Among the identified isomers,  $^1\text{SS}(=\text{O})=\text{O}$  is at the lowest energy with  $-42.69 \text{ kcal}\cdot\text{mol}^{-1}$ . For each of these isomers, the energy of the triplet configuration has also been calculated. The data show that all energies of the triplet state isomers are significantly higher than that of the singlets.

The remaining three isomers reported in this study are cyclic structures,  $^1\text{Y}(\text{SOO}) = \text{S}$  at  $24.89 \text{ kcal}\cdot\text{mol}^{-1}$  and  $^1\text{Y}(\text{SSOO})$  at a higher energy of  $54.28 \text{ kcal}\cdot\text{mol}^{-1}$ . We note that Marsden and Smith [5] have also identified and reported the optimized geometries of these cyclic structures, however, the authors are not aware of any studies that have estimated the enthalpies of these compounds. Examination of the CBS-QB3, G3B3 and G4 optimized geometries (bond length and angle) are in very good agreement with those reported in ref. [5]. Comparisons of the geometries are reported in the supplemental material.





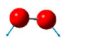

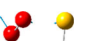
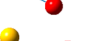
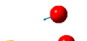


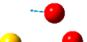
Table 3 lists the standard enthalpies  $\Delta H_{TS}$  of 18 transition state structures in the  $^3\text{S}_2 + ^3\text{O}_2$  reaction system. The structures of the identified transition states are also illustrated in Table 3 along with the paths from reactant to product/intermediate. Except for one transition state (TS3-8, see Table 3), the results of G4 calculations are recommended values. The enthalpies of the transition states are calculated from both the reactant and the product side. Comparison to literature values was possible for a number of TS-structures. These include TS3-1, TS3-8, TS3-9, TS3-11, and T3-12 where good agreement is obtained with refs. [8,13], showing a deviation of  $3\text{--}4 \text{ kcal}\cdot\text{mol}^{-1}$ . Unfortunately and in contrast to the compounds listed in Table 2, the calculation of four transition state structures could not be identified and evaluated with the W1U method.

To verify the calculated energy of the transition states (*trans*- and *cis*-configurations) of the reaction system  $^3\text{S}_2 + ^3\text{O}_2$  an additional series of calculations has been executed. Using different estimated geometries, frequency calculations have been performed at different given S–O bond lengths until an imaginary frequency was found. For each calculation, the S–O length value was frozen. With the help of GaussView each structure has been examined and several structures were selected for a full ab-initio energy calculation. In the example illustrated in Table 4, CBS-QB3 calculations resulted in the lowest energy for the transition state structure for *cis*- $^1\text{SSOO}$  formation at  $2.35 \text{ \AA}$  S–O bond length. The energy calculated at  $2.35 \text{ \AA}$  is then used for the determination of the TS enthalpy. The same calculations were made for G3B3, G4 and W1U as far as computational capacities were available.

The calculations have further brought about that the *cis*-configuration adduct of  $^3\text{O}_2$  on  $^3\text{S}_2$  is lower by ca.  $10 \text{ kcal}\cdot\text{mol}^{-1}$  and therefore energetically more favorable than the

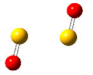
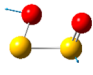
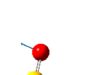

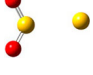
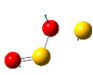

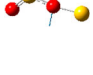

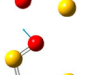
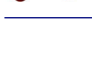
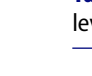
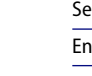
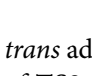
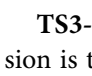


**Table 3.** Calculated enthalpies at 298 K for transition state structures in the  $^3\text{S}_2 + ^3\text{O}_2$  system in kcal·mol $^{-1}$  ( $\Delta H_{\text{TS}}$ ).

Transition state structure	Reactants → TS TS → Products	Δ <i>H</i> <sub>TS</sub> in kcal·mol <sup>−1</sup>			
		CBS-QB3	G3B3	G4	W1U
<sup>3</sup> S <sub>2</sub> + <sup>3</sup> O <sub>2</sub> → <i>trans</i> - <sup>1</sup> SSOO → Products					
	<sup>3</sup> S <sub>2</sub> + <sup>3</sup> O <sub>2</sub> → <sup>1</sup> <b>TS1</b>	40.44	41.59	43.58	45.20
	<sup>1</sup> <b>TS1</b> → <i>trans</i> - <sup>1</sup> SSOO	38.81	40.45	42.88	43.85
	Average	39.63	41.02	<b>43.23</b>	44.53
	<i>trans</i> - <sup>1</sup> SSOO → <sup>1</sup> <b>TS1-1</b>	41.73	44.41	42.77	47.05
	<sup>1</sup> <b>TS1-1</b> → <sup>1</sup> Y(SOO) = S	40.23	43.06	41.97	46.12
	Average	40.98	43.73	<b>42.37</b>	46.58
	<sup>1</sup> Y(SOO) = S → <sup>1</sup> <b>TS1-2</b>	34.75	25.70	30.51	37.22
	<sup>1</sup> <b>TS1-2</b> → <sup>1</sup> SS(=O) = O	34.75	25.70	30.51	37.22
	Average	34.75	25.70	<b>30.51</b>	37.22
	<sup>1</sup> SS(=O) = O → <sup>1</sup> <b>TS1-3</b>	20.77	19.93	21.56	23.63
	<sup>1</sup> <b>TS1-3</b> → <sup>1</sup> SO <sub>2</sub> + <sup>3</sup> S	21.68	21.03	22.64	24.60
	Average	21.23	20.48	<b>22.10</b>	24.12
<sup>3</sup> S <sub>2</sub> + <sup>3</sup> O <sub>2</sub> → <sup>1</sup> Y(SSOO) → Products					
	<sup>3</sup> S <sub>2</sub> + <sup>3</sup> O <sub>2</sub> → <sup>1</sup> <b>TS2</b>	77.29	82.21	75.74	–
	<sup>1</sup> <b>TS2</b> → <sup>1</sup> Y(SSOO)	75.32	80.32	74.61	–
	Average	76.31	81.27	<b>75.17</b>	–
	<sup>1</sup> Y(SSOO) → <sup>1</sup> <b>TS2-1</b>	61.22	62.18	60.25	61.17
	<sup>1</sup> <b>TS2-1</b> → <i>cis</i> - <sup>1</sup> OSSO	62.35	63.75	60.69	61.92
	Average	61.79	62.97	<b>60.47</b>	61.55
<sup>3</sup> S <sub>2</sub> + <sup>3</sup> O <sub>2</sub> → <i>cis</i> - <sup>1</sup> SSOO → Products					
	<sup>3</sup> S <sub>2</sub> + <sup>3</sup> O <sub>2</sub> → <sup>1</sup> <b>TS3</b>	40.44	42.58	40.49	44.25
	<sup>1</sup> <b>TS3</b> → <i>cis</i> - <sup>1</sup> SSOO	38.81	41.44	39.79	42.89
	Average	39.63	42.01	<b>40.14</b>	43.57
	<i>cis</i> - <sup>1</sup> SSOO → <sup>1</sup> <b>TS3-1</b>	93.87	95.13	94.50	94.38
	<sup>1</sup> <b>TS3-1</b> → <sup>1</sup> SSO + <sup>3</sup> O	91.46	92.68	92.61	92.57
	Average	92.66	93.91	<b>93.55</b>	93.48
	Ref. [13]: 99.22				
	<i>cis</i> - <sup>1</sup> SSOO → <sup>1</sup> <b>TS3-2</b>	28.52	–	32.58	–
	<sup>1</sup> <b>TS3-2</b> → <sup>1</sup> Y(SOO) = S	27.03		30.77	
	Average	27.78		<b>31.17</b>	
	<sup>1</sup> Y(SOO) = S → <sup>1</sup> <b>TS3-3</b>	34.75	25.70	30.51	37.22
	<sup>1</sup> <b>TS3-3</b> → <sup>1</sup> SS(=O) = O	34.75	25.70	30.51	37.22
	Average	34.75	25.70	<b>30.51</b>	37.22
	<sup>1</sup> SS(=O) = O → <sup>1</sup> <b>TS3-4</b>	20.77	19.93	21.56	23.63
	<sup>1</sup> <b>TS3-4</b> → <sup>1</sup> SO <sub>2</sub> + <sup>3</sup> S	21.68	21.03	22.64	24.60
	Average	21.23	20.48	<b>22.10</b>	24.12
	<i>cis</i> - <sup>1</sup> SSOO → <sup>1</sup> <b>TS3-5</b>	66.37	72.84	67.91	70.76
	<sup>1</sup> <b>TS3-5</b> → <i>cis</i> - <sup>1</sup> OSSO	67.17	73.66	68.54	71.36
	Average	66.77	73.25	<b>68.23</b>	71.06

(continued).

**Table 3.** Continued.

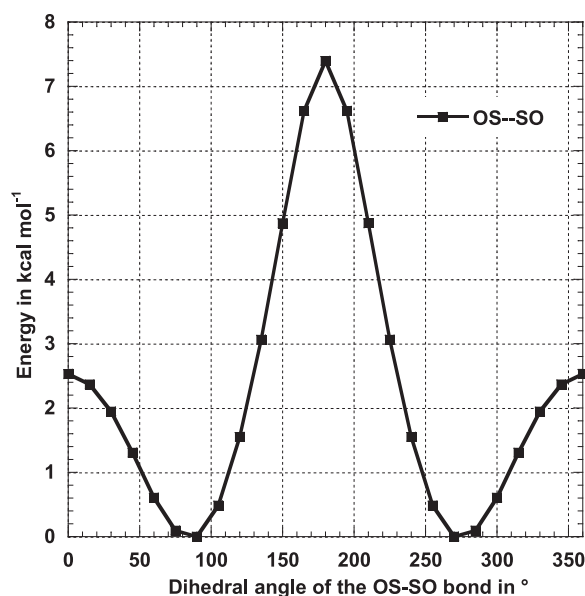
Transition state structure	Reactants → TS TS → Products	$\Delta H_{TS}$ in kcal·mol <sup>-1</sup>			
		CBS-QB3	G3B3	G4	W1U
	Calculated with Rotor				
	<i>cis</i> - <sup>1</sup> OSSO → <sup>1</sup> <b>TS3-6</b>			<b>-22.3</b>	-3.62 [8]
	<sup>1</sup> <b>TS3-6</b> → <i>trans</i> - <sup>1</sup> OSSO				
	<i>trans</i> - <sup>1</sup> OSSO → <sup>1</sup> <b>TS3-7</b>	2.62	3.88	3.30	-
	<sup>1</sup> <b>TS3-7</b> → 2 <sup>3</sup> SO	3.28	4.63	3.58	
	Average	2.95	4.26	<b>3.44</b>	
	<i>cis</i> - <sup>1</sup> OSSO → <sup>1</sup> <b>TS3-8</b>	3.85	8.30	-1.42	9.38
	<sup>1</sup> <b>TS3-8</b> → <sup>1</sup> Y(SSO) = O	1.55	6.13	-1.93	7.93
	Average	2.70	<b>7.22</b>	-1.68	8.65
	Ref. [13]: 5.59; Ref. [8]: 4.20				
	<sup>1</sup> Y(SSO) = O → <sup>1</sup> <b>TS3-9</b>	5.33	4.63	4.21	6.19
	<sup>1</sup> <b>TS3-9</b> → <sup>1</sup> SS(=O) = O	5.33	4.63	4.21	6.19
	Average	5.33	4.63	<b>4.21</b>	6.19
	Ref. [13]: 5.6				
	<sup>1</sup> SS(=O) = O → <sup>1</sup> <b>TS3-10</b>	20.77	19.93	21.56	23.63
	<sup>1</sup> <b>TS3-10</b> → <sup>1</sup> SO <sub>2</sub> + <sup>3</sup> S	21.68	21.03	22.64	24.60
	Average	21.23	20.48	<b>22.10</b>	24.12
	<sup>1</sup> Y(SSO) = O → <sup>1</sup> <b>TS3-11</b>	-3.62	-3.64	-3.71	-1.53
	<sup>1</sup> <b>TS3-11</b> → <i>trans</i> - <sup>1</sup> SOSO	-0.91	-1.47	-2.28	-0.08
	Average	-2.26	-2.55	<b>-3.00</b>	-0.80
	Ref. [13]: -1.69; Ref. [8]: -1.36				
	<i>trans</i> - <sup>1</sup> SOSO → <sup>1</sup> <b>TS3-12</b>	6.09	5.91	4.10	6.05
	<sup>1</sup> <b>TS3-12</b> → <i>cis</i> - <sup>1</sup> SOSO	5.67	5.91	4.10	6.05
	Average	5.88	5.91	<b>4.10</b>	6.05
	Ref. [13]: 5.53; Ref. [8]: 9.51				
	<i>cis</i> - <sup>1</sup> SOSO → <sup>1</sup> <b>TS3-13</b>	-3.42	2.18	-2.41	-
	<sup>1</sup> <b>TS3-13</b> → 2 <sup>3</sup> SO	-2.92	-1.43	-2.13	
	Average	-3.21	-1.80	<b>-2.27</b>	
	<i>cis</i> - <sup>1</sup> SOSO → <sup>1</sup> <b>TS3-14</b>	22.75	22.98	24.29	<b>G3</b> 21.04
	<sup>1</sup> <b>TS3-14</b> → <sup>1</sup> SO <sub>2</sub> + <sup>3</sup> S	21.35	21.91	23.93	20.62
	Average	22.05	22.44	<b>24.11</b>	20.83

**Table 4.** Calculation of transition state <sup>1</sup>**TS3** energy for *cis*-<sup>1</sup>SSOO formation on CBS-QB3 level.

Selected S–O in Å	CBS-QB3			
	2.0	2.35	2.5	2.7
Energy in Hartrees	–946.272836	<b>–945.573903</b>	–945.564148	–945.563494

*trans* adduct. The same calculations have been performed for the transition state structure of **TS3-7** for the dissociation of *trans*-<sup>1</sup>OSSO to 2<sup>3</sup>SO.

**TS3-1** and **TS3-5** (see Table 3) exhibit similar structures, in which O–O bond scission is taking place, but the corresponding enthalpies of these transition states differ by



**Figure 1.** Rotational barrier of  $^1\text{OSSO}$  about OS–SO bond. The *cis*- and *trans*- structures are illustrated in Figure 2.

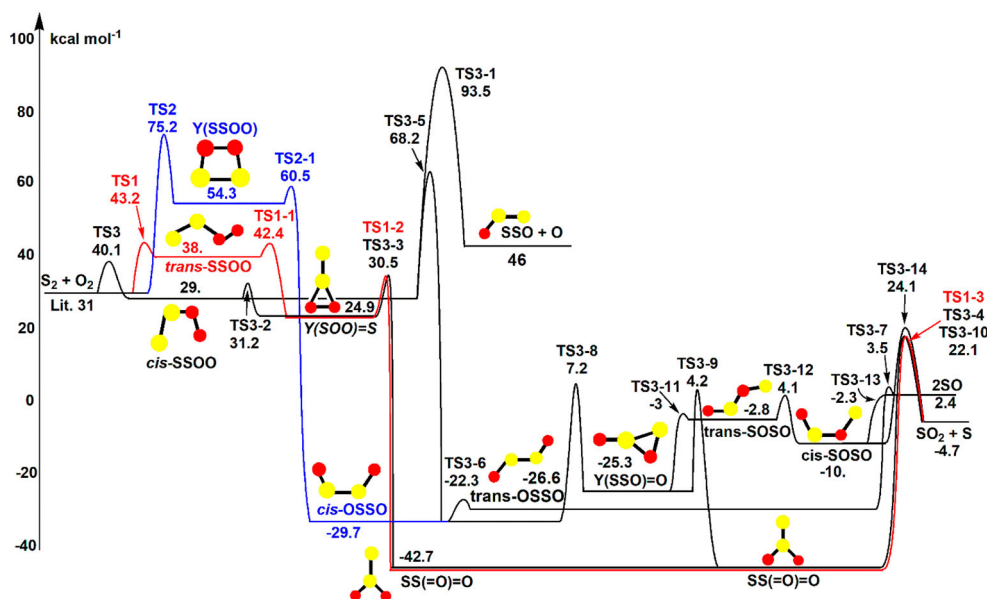
$26 \text{ kcal}\cdot\text{mol}^{-1}$ . In **TS3-5**, one oxygen undergoes an intramolecular isomerization by moving to the sulfur atom to form *cis*- $^1\text{OSSO}$ , while in **TS3-1**, a bond scission is observed resulting in  $^1\text{SSO}$  and an oxygen atom.

Further calculations have been performed for the determination of the energy barrier necessary for the conversion of *cis*- $^1\text{OSSO}$  to *trans*- $^1\text{OSSO}$  (**TS3-6**) via internal rotation. The potential barrier versus torsion angle for internal rotation of OS–SO on the B3LYP/6-31G(d,p) level was calculated. The potential energy as a function of dihedral angle is determined by rotating the molecule about the S–S bond from  $0^\circ$  to  $360^\circ$  at  $15^\circ$  intervals and by optimizing each new structure as illustrated in Figure 1. The barriers for internal rotation are calculated from the differences between the maxima and the minima of the total energy of the structures. The highest rotation barrier relative to *cis*- $^1\text{OSSO}$  is at  $7.4 \text{ kcal}\cdot\text{mol}^{-1}$  so that the energy barrier of the transition state **TS3-6** is therefore  $-22.3 \text{ kcal}\cdot\text{mol}^{-1}$ .

The **TS3-2** transition state structure resulting from the further reaction of *cis*- $^1\text{SSOO}$  exhibits two sets of values corresponding to the applied methods.  $27.78$  and  $31.17 \text{ kcal}\cdot\text{mol}^{-1}$  have been calculated on CBS-QB3 and G4 level, respectively, while G3B3 and W1U calculations have identified a different structure at a higher energy which is not considered in this study. Examination of the reaction that converts the *trans*- $^1\text{SSOO}$  to the cyclic  $^1\text{Y}(\text{SOO}) = \text{S}$  isomer (**TS1-1**) results in a low barrier of some  $4 \text{ kcal}\cdot\text{mol}^{-1}$ . Therefore and by analogy, for the reaction of the *cis*- $^1\text{SSOO}$  structure (in which the bond lengths are similar) to the  $^1\text{Y}(\text{SOO}) = \text{S}$  isomer, we recommend the lower barrier obtained with G4 and CBS-QB3. To support this choice, reaction enthalpies have been examined. Table 5 lists the reaction enthalpies of reactions *cis*- $^1\text{SSOO} \rightarrow \text{TS3-2}$  (R1) and *trans*- $^1\text{SSOO} \rightarrow \text{TS1-1}$  (R2) for the four methods. The results show similar reaction enthalpies for R1 and R2 when using both G4 and CBS-QB3.

**Table 5.** Reaction enthalpy comparisons in kcal·mol<sup>-1</sup>.

	R1: <i>cis</i> - <sup>1</sup> SSOO → <b>TS3-2</b>	R2: <i>trans</i> - <sup>1</sup> SSOO → <b>TS1-1</b>
CBS-QB3	1.408	0.636
G3B3	-30.742	7.796
G4	-2.5	4.763
W1U	-23.918	6.615

**Figure 2.** Potential diagram for reactions of the <sup>3</sup>S<sub>2</sub> + <sup>3</sup>O<sub>2</sub> reaction system. Values represent the recommended enthalpies in kcal·mol<sup>-1</sup> as listed in Tables 2 and 3. Electron spin multiplicity as given in Tables 2 and 3.

In comparison, the corresponding reaction enthalpies estimated with G3B3 and W1U exhibit a large difference between R1 and R2. These observations support the enthalpy of **TS3-2** of 31.2 kcal·mol<sup>-1</sup> being similar to that of **TS1-1**.

### 3.2. Reactions and potential energy diagram for the <sup>3</sup>S<sub>2</sub> + <sup>3</sup>O<sub>2</sub> reaction system

Figure 2 illustrates the major channels for the <sup>3</sup>S<sub>2</sub> + <sup>3</sup>O<sub>2</sub> reactions. There are three initial addition reactions, each path having a significant energy barrier: Addition of an oxygen atom to one sulfur atom with the oxygen molecule in *cis* or *trans* position to the terminal sulfur atom leads to *cis*-<sup>1</sup>SSOO and *trans*-<sup>1</sup>SSOO intermediates, respectively, with barriers of 9.1 and 12.2 kcal·mol<sup>-1</sup> relative to the entrance channel which is at 31 kcal·mol<sup>-1</sup>. The third path involves the formation of a cyclic <sup>1</sup>Y(SSOO) with each oxygen bonding to a different sulfur over a barrier of 44.2 kcal·mol<sup>-1</sup> relative to the entrance channel. The *cis*- and *trans*-isomers as well as <sup>1</sup>Y(SSOO) recombine at different levels of energy to form the stable <sup>1</sup>SS(=O)=O (SSO<sub>2</sub>) molecule or dissociate to 2 <sup>3</sup>SO. The different reaction pathways are detailed in Table 3 and discussed in the following sections.

### 3.2.1. Addition of $^3\text{O}_2$ to $^3\text{S}_2$ and $\text{trans}^{-1}\text{SSOO}$ formation

The  $\text{trans}^{-1}\text{SSOO}$  isomer is formed after overcoming approximately  $12\text{ kcal}\cdot\text{mol}^{-1}$  (TS1) relative to the entrance channel (at  $31\text{ kcal}\cdot\text{mol}^{-1}$ ) and opening the double bond of the  $^3\text{S}_2$  molecule. A successive reaction identified for this  $\text{trans}^{-1}\text{SSOO}$  isomer formed at  $38\text{ kcal}\cdot\text{mol}^{-1}$  consists in a ring closure (TS1-1) delivering the 3-membered  $^1\text{Y}(\text{SOO}) = \text{S}$  molecule at  $24.9\text{ kcal}\cdot\text{mol}^{-1}$ , in which the two oxygens are part of the ring. The strained cyclic  $^1\text{Y}(\text{SOO}) = \text{S}$  opens the ring by breaking the O–O bond (TS1-2) over a low barrier of ca.  $6\text{ kcal}\cdot\text{mol}^{-1}$  relative to the  $^1\text{Y}(\text{SOO}) = \text{S}$  isomer. This low barrier is partially due to release of the strain in the three membered ring. The new compound is a stable low-energy compound  $^1(\text{SS}(=\text{O})=\text{O})$  formed with an excess energy of  $68\text{ kcal}\cdot\text{mol}^{-1}$  relative to cyclic isomer  $^1\text{Y}(\text{SOO}) = \text{S}$ . This path has not been reported in the literature.

We note that Goodazi *et al.* [13] report  $\text{trans}^{-1}\text{SOSO}$  formation from  $\text{trans}^{-1}\text{SSOO}$ , however, their calculations show that this reaction occurs over two relatively high, double barriers of  $149\text{ kcal}\cdot\text{mol}^{-1}$  and  $132\text{ kcal}\cdot\text{mol}^{-1}$  or  $113\text{ kcal}\cdot\text{mol}^{-1}$  relative to  $\text{trans}^{-1}\text{SSOO}$ . This path is not considered in this study. Further dissociation of the stable  $^1\text{SS}(=\text{O})=\text{O}$  isomer (TS1-3) leads to  $^1\text{SO}_2 + ^3\text{S}$  over a high barrier of  $65\text{ kcal}\cdot\text{mol}^{-1}$  over to  $^1\text{SS}(=\text{O})=\text{O}$ .

### 3.2.2. Addition of $^3\text{O}_2$ on $^3\text{S}_2$ to form a cyclic 4-membered $^1\text{Y}(\text{SSOO})$ isomer

Figure 2 illustrates the formation of a 4-membered ring from the simultaneous addition of each oxygen atom onto each sulfur atom. The barrier for this reaction is calculated to be  $44.2\text{ kcal}\cdot\text{mol}^{-1}$  (TS2), relative to the entrance channel at  $31\text{ kcal}\cdot\text{mol}^{-1}$ . This isomer is relatively unstable at  $54.3\text{ kcal}\cdot\text{mol}^{-1}$  and undergoes ring opening by cleaving the O–O bond (TS2-1) over a low barrier of  $6.2\text{ kcal}\cdot\text{mol}^{-1}$ , relative to the cyclic  $^1\text{Y}(\text{SSOO})$ , resulting in a more stable  $\text{cis}^{-1}\text{OSSO}$  at  $-29.7\text{ kcal}\cdot\text{mol}^{-1}$ . Two further reaction pathways of the formed  $\text{cis}^{-1}\text{OSSO}$  isomer are discussed in section 2.3 below.

### 3.2.3. Addition of $^3\text{O}_2$ to $^3\text{S}_2$ and $\text{cis}^{-1}\text{SSOO}$ formation

The addition of  $^3\text{O}_2$  to  $^3\text{S}_2$  in a  $\text{cis}$ -configuration occurs with a barrier of  $9.1\text{ kcal}\cdot\text{mol}^{-1}$  (TS3) above the entrance channel which lies at  $31\text{ kcal}\cdot\text{mol}^{-1}$ ; the  $\text{cis}^{-1}\text{SSOO}$  radical formed is evaluated at  $29\text{ kcal}\cdot\text{mol}^{-1}$  which is slightly lower than that of the entrance channel. Figure 2 and Table 3 illustrate the reaction paths and corresponding energies.

One forward reaction of this  $\text{cis}^{-1}\text{SSOO}$  isomer has been identified through (TS3-1) where the imaginary frequency shows the terminal oxygen leaving the  $\text{cis}^{-1}\text{SSOO}$  radical resulting in  $^1\text{SSO} + ^3\text{O}$  at  $46\text{ kcal}\cdot\text{mol}^{-1}$ . This dissociation reaction requiring ca.  $63\text{ kcal}\cdot\text{mol}^{-1}$  above the entrance channel was readily identified with all the calculation methods used. The calculated enthalpy value as well as the geometry of this transition state structure (TS3-1) are in good agreement with the literature value reported in [13] (see Table 3).

A different path for the  $\text{cis}^{-1}\text{SSOO}$  peroxide consists of an intramolecular attack of the terminal oxygen on the centered sulfur atom almost without barrier, viz.  $2.2\text{ kcal}\cdot\text{mol}^{-1}$  (TS3-2) above  $\text{cis}^{-1}\text{SSOO}$ , calculated on G4 level. This pathway involves the formation of a 3-membered ring, bonding the terminal oxygen atom to the sulfur. The resulting cyclic compound formed through this intramolecular addition, ( $^1\text{Y}(\text{SOO}) = \text{S}$ ) at  $24.9\text{ kcal}\cdot\text{mol}^{-1}$  is the same isomer as that formed through  $\text{trans}^{-1}\text{SSOO}$  isomer ring closure. Marsden and Smith [5] have identified and reported this cyclic isomer. Examination

of the geometries (bond lengths and angles) show that the S = S bond length is 1.89 Å calculated with CBS-QB3 and G4 versus 1.86 Å in ref. [5]. The S–O bond lengths from G4/CBS-QB3 calculations are 1.67 Å and 1.70 Å, respectively, versus 1.675 in [5]. The SSO angle with 113.6 degrees for both methods is also in good agreement with 113.0 degrees from literature. The OSO angles calculated in this study are 52.47/53.3 degrees, deviating by ca. 2.5 degrees from that of Ref. [5] with 55.1 degrees. This cyclic  $^1\text{Y}(\text{SOO}) = \text{S}$  compound will then open the SOO-ring via cleavage of the O–O bond (**TS3-3**) leading to the stable  $^1\text{SS}(=\text{O}) = \text{O}$  at  $-42.7 \text{ kcal}\cdot\text{mol}^{-1}$  and releasing an excess of energy. The available energy forces for the dissociation reaction to  $^1\text{SO}_2 + ^3\text{S}$  through a ca.  $65 \text{ kcal}\cdot\text{mol}^{-1}$  barrier (**TS3-4**) relative to  $^1\text{SS}(=\text{O}) = \text{O}$ .

In the third channel the *cis*- $^1\text{SSOO}$  isomer undergoes an oxygen-intramolecular atom transfer, in which the terminal oxygen moves to the terminal sulfur forming a *cis*- $^1\text{OSSO}$  isomer. To take place, this transition state structure (**TS3-5**) requires an energy of  $39.2 \text{ kcal}\cdot\text{mol}^{-1}$  above the *cis*-SSOO compound. The formation of the *cis*- $^1\text{OSSO}$  at  $-29.7 \text{ kcal}\cdot\text{mol}^{-1}$  is exothermic by ca.  $59 \text{ kcal}\cdot\text{mol}^{-1}$  and provides excess of energy for the *cis*- $^1\text{OSSO}$  to react further.

Two successive paths are available to the *cis*- $^1\text{OSSO}$  isomer: The first one is a rearrangement over a small barrier (**TS3-6**) of  $7.4 \text{ kcal}\cdot\text{mol}^{-1}$  to *trans*- $^1\text{OSSO}$  which can further dissociate to 2  $^3\text{SO}$  molecules (**TS3-7**). The second reaction path of the *cis*- $^1\text{OSSO}$  leads to a O–S bond formation over a  $36.9 \text{ kcal}\cdot\text{mol}^{-1}$  barrier (**TS3-8**) relative to *cis*- $^1\text{OSSO}$  to a new stable cyclic compound  $^1\text{Y}(\text{SSO}) = \text{O}$  at  $-25.3 \text{ kcal}\cdot\text{mol}^{-1}$ . This barrier is in agreement with the value reported in Ref. [13].  $^1\text{Y}(\text{SSO}) = \text{O}$  undergoes further ring opening via two paths: Cleavage of the S–O bond over some  $30 \text{ kcal}\cdot\text{mol}^{-1}$  energy barrier (**TS3-9**) over  $^1\text{Y}(\text{SSO}) = \text{O}$  to form the stable  $^1\text{SS}(=\text{O}) = \text{O}$  compound which may dissociate to  $^1\text{SO}_2 + ^3\text{S}$  (**TS3-10**). Alternately,  $^1\text{Y}(\text{SSO}) = \text{O}$  can cleave the S–S bond over a  $22.3 \text{ kcal}\cdot\text{mol}^{-1}$  barrier (**TS3-11**) to form a *trans*- $^1\text{SOSO}$  isomer. This last radical rearranges (**TS3-12**) to the formation of *cis*- $^1\text{SOSO}$  lying at  $-10 \text{ kcal}\cdot\text{mol}^{-1}$ . *Cis*- $^1\text{SOSO}$  dissociates via two paths: One governed by a barrierless dissociation to 2  $^3\text{SO}$  (**TS3-13**) and the second through an energy barrier of  $34.1 \text{ kcal}\cdot\text{mol}^{-1}$  relative to *cis*- $^1\text{SOSO}$  (**TS3-14**) to the set of products  $^1\text{SO}_2 + ^3\text{S}$ .

### 3.3. Kinetic calculations for $^3\text{S}_2 + ^3\text{O}_2$

Multi-channel, multi-frequency QRRK [25,26] calculations are performed for  $k(E)$  with master equation analysis CHEMASTER code [27,28] for the  $^3\text{S}_2 + ^3\text{O}_2$  reaction system to estimate rate coefficients and to determine important reaction paths as a function of temperature and pressure.

Three wells are considered for the formation of intermediates in the reaction of  $^3\text{S}_2 + ^3\text{O}_2$ : the ring formation, the addition to the *trans*-configuration and the addition to the *cis*-configuration. These three intermediates undergo isomerization or dissociation reactions as illustrated in Figure 2. The calculations provide sets of rate coefficients  $k(T)$  for the stabilization of the formed adducts and reaction products of successive reactions at different temperatures and pressures.

Tables 6–8 list calculated high-pressure-limit kinetic parameters for the reactions illustrated in Figure 2. The input data to the QRRK / Master Equation analysis are reaction equations together with enthalpies, frequencies, moment of inertia, see [28]. Both forward

**Table 6.** Reaction rate coefficients from QRRK calculations<sup>a</sup>:  $^3S_2 + ^3O_2 \rightarrow ^1Y(SSOO)$  channel.

Reactions	A	n	E <sub>A</sub> (kcal·mol <sup>-1</sup> )
$^3S_2 + ^3O_2 \rightarrow ^1Y(SSOO) \rightarrow \text{Products}$			
$^3S_2 + ^3O_2 \rightarrow ^1Y(SSOO)$	2.76E + 04	2.11	44.34
$^1Y(SSOO) \rightarrow ^3S_2 + ^3O_2$	1.66E + 13	0.21	21.43
$^1Y(SSOO) \rightarrow \text{cis-}^1OSSO$	6.89E + 12	0.022	6.78
$\text{cis-}^1OSSO \rightarrow ^1Y(SSOO)$	4.35E + 11	0.21	90.62
$\text{cis-}^1OSSO \rightarrow \text{trans-}^1OSSO$	3.09E + 18	-2.01	9.26
$\text{cis-}^1OSSO \rightarrow ^1Y(SSO) = O$	3.94E + 11	0.39	28.36
$^1Y(SSO) = O \rightarrow \text{cis-}^1OSSO$	2.05E + 12	0.28	22.73
$^1Y(SSO) = O \rightarrow ^1SS(=O) = O$	3.99E + 12	0.21	29.97
$^1SS(=O) = O \rightarrow ^1Y(SSO) = O$	1.28E + 12	0.43	47.32
$^1SS(=O) = O \rightarrow ^1SO_2 + ^3S$	9.83E + 16	-0.79	65.98
$\text{trans-}^1SOSO \rightarrow ^1Y(SSO) = O$	1.12E + 12	0.19	0.31
$\text{trans-}^1SOSO \rightarrow \text{cis-}^1SOSO$	2.05E + 12	0.16	7.42
$\text{cis-}^1SOSO \rightarrow \text{trans-}^1SOSO$	2.10E + 12	0.22	14.48
$\text{cis-}^1SOSO \rightarrow 2^3SO$	1.09E + 12	0.23	8.09
$\text{cis-}^1SOSO \rightarrow ^1SO_2 + ^3S$	2.16E + 13	-0.01	34.58
$\text{trans-}^1OSSO \rightarrow \text{cis-}^1OSSO$	3.09E + 18	-2.01	9.26
$\text{trans-}^1OSSO \rightarrow 2^3SO$	4.20E + 18	-2.04	31.90

<sup>a</sup>The units of A factors and rate constants k are s<sup>-1</sup> for unimolecular reactions and cm<sup>3</sup> mol<sup>-1</sup> sec<sup>-1</sup> for bimolecular reactions. <sup>1</sup>X = singlet, <sup>3</sup>X = triplet.

**Table 7.** Reaction rate coefficients from QRRK calculations<sup>a</sup>:  $^3S_2 + ^3O_2 \rightarrow \text{trans-}^1SSOO$  channel.

Reactions	A	n	E <sub>A</sub> (kcal·mol <sup>-1</sup> )
$^3S_2 + ^3O_2 \rightarrow \text{trans-}^1SSOO \rightarrow \text{Products}$			
$^3S_2 + ^3O_2 \rightarrow \text{trans-}^1SSOO$	7.82E + 06	1.09	13.02
$\text{trans-}^1SSOO \rightarrow ^3S_2 + ^3O_2$	9.64E + 14	-0.80	6.33
$\text{trans-}^1SSOO \rightarrow ^1Y(SOO) = S$	2.11E + 12	0.13	4.88
$^1Y(SOO) = S \rightarrow \text{trans-}^1SSOO$	6.24E + 12	0.15	18.03
$^1Y(SOO) = S \rightarrow ^1SS(=O) = O$	1.52E + 13	0.14	6.18
$^1SS(=O) = O \rightarrow ^1Y(SOO) = S$	2.22E + 12	0.50	73.62
$^1SS(=O) = O \rightarrow ^1SO_2 + ^3S$	9.83E + 16	-0.79	65.98

<sup>a</sup>The units of A factors and rate constants k are s<sup>-1</sup> for unimolecular reactions and cm<sup>3</sup> mol<sup>-1</sup> sec<sup>-1</sup> for bimolecular reactions. <sup>1</sup>X = singlet; <sup>3</sup>X = triplet.

and backward reactions are given in Tables 6–8. Data reported in the study of Frandsen *et al.* [8] are also used to calculate the corresponding kinetic parameters and are listed in Table 8 as well for comparison.

Figures 3–5 illustrate the calculated temperature dependent rate coefficients resulting from the master equation predictions for the formation and consecutive reactions of *cis*-<sup>1</sup>SSOO, <sup>1</sup>Y(SSOO) and *trans*-<sup>1</sup>SSOO intermediates at a constant pressure of 1 atm.

The reaction rate coefficients at *P* = 1 atm represented in Figure 3 illustrate the formation of *cis*-<sup>1</sup>SSOO and the final products from consecutive reactions of the *cis*-<sup>1</sup>SSOO intermediate. The reaction rate coefficients for the formation of all species except for the formation of *cis*-<sup>1</sup>SSOO gain in importance as temperature increases. Since <sup>1</sup>SS(=O) = O, <sup>3</sup>SO and <sup>1</sup>SO<sub>2</sub> + <sup>3</sup>S are each formed through two different channels, the sum of rate coefficients of both channels is given in Figure 3.



**Table 8.** Reaction rate coefficients from QRRK calculations<sup>a</sup>:  $^3\text{S}_2 + ^3\text{O}_2 \rightarrow \text{cis-}^1\text{SSOO}$  channel.

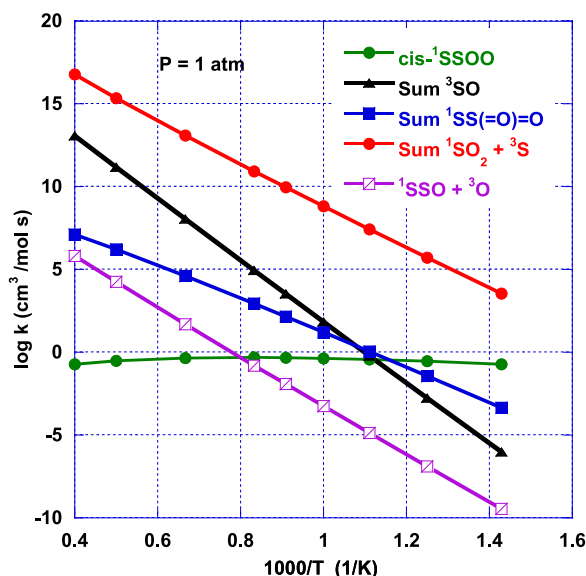
Reactions	A	n	$E_A(\text{kcalmol}^{-1})$
$^3\text{S}_2 + ^3\text{O}_2 \rightarrow \text{cis-}^1\text{SSOO} \rightarrow \text{Products}$			
$^3\text{S}_2 + ^3\text{O}_2 \rightarrow \text{cis-}^1\text{SSOO}$	1.78E+04	2.11	9.26
$\text{cis-}^1\text{SSOO} \rightarrow ^3\text{S}_2 + ^3\text{O}_2$	2.05E+12	0.29	11.53
$\text{cis-}^1\text{SSOO} \rightarrow ^1\text{Y}(\text{SOO}) = \text{S}$	1.70E+12	.25088	2.62
$\text{cis-}^1\text{SSOO} \rightarrow \text{cis-}^1\text{OSSO}$	2.37E+12	0.26	39.67
$\text{cis-}^1\text{SSOO} \rightarrow ^1\text{SSO} + ^3\text{O}$	3.94E+12	0.24	64.98
$^1\text{Y}(\text{SOO}) = \text{S} \rightarrow \text{cis-}^1\text{SSOO}$	5.37E+12	0.20	6.81
$^1\text{Y}(\text{SOO}) = \text{S} \rightarrow ^1\text{SS}(=\text{O}) = \text{O}$	1.5E+13	0.14	6.18
$^1\text{SS}(=\text{O}) = \text{O} \rightarrow ^1\text{Y}(\text{SOO}) = \text{S}$	2.22E+12	0.50	73.62
$^1\text{SS}(=\text{O}) = \text{O} \rightarrow ^1\text{SO}_2 + ^3\text{S}$	9.83E+16	-0.79	65.98
$\text{cis-}^1\text{OSSO} \rightarrow \text{cis-}^1\text{SSOO}$	7.84E+11	0.37	98.33
$\text{cis-}^1\text{OSSO} \rightarrow ^1\text{Y}(\text{SSO}) = \text{O}$	3.94E+11	0.39	28.36
$\text{cis-}^1\text{OSSO} \rightarrow \text{trans-}^1\text{OSSO}$	3.09E+18	-2.01	9.26
Ref. [8]	1.94E+18	-1.90	22.28
$^1\text{Y}(\text{SSO}) = \text{O} \rightarrow \text{cis-}^1\text{SOSO}$	1.73E+12	0.38	23.98
$^1\text{Y}(\text{SSO}) = \text{O} \rightarrow \text{trans-}^1\text{SOSO}$	2.05E+12	0.28	22.72
Ref. [8]	1.31E+12	0.43	17.17
$^1\text{Y}(\text{SSO}) = \text{O} \rightarrow ^1\text{SS}(=\text{O}) = \text{O}$	3.99E+12	0.210.36	29.97
Ref. [8]	2.25E+12		30.45
$\text{trans-}^1\text{SOSO} \rightarrow ^1\text{Y}(\text{SSO}) = \text{O}$	1.12E+12	0.19	0.307
Ref. [8]	2.88E+11	0.36	0.523
$\text{trans-}^1\text{SOSO} \rightarrow \text{cis-}^1\text{SOSO}$	2.05E+12	0.16	7.42
Ref. [8]	3.22E+11	0.41	11.35
$\text{cis-}^1\text{SOSO} \rightarrow \text{trans-}^1\text{SOSO}$	2.10E+12	0.22	14.48
Ref. [8]	6.77E+11	0.46	14.94
$\text{cis-}^1\text{SOSO} \rightarrow 2^3\text{SO}$	1.10E+12	0.23	8.09
$\text{cis-}^1\text{SOSO} \rightarrow ^1\text{SO}_2 + ^3\text{S}$	2.17E+13	-0.009	34.58
$\text{trans-}^1\text{OSSO} \rightarrow \text{cis-}^1\text{OSSO}$	3.09E+18	-2.01	9.257
Ref. [8]	1.75E+18	-1.96	20.10
$\text{trans-}^1\text{OSSO} \rightarrow 2^3\text{SO}$	4.20E+18	-2.04	31.90

<sup>a</sup>The units of A factors and rate constants k are  $\text{s}^{-1}$  for unimolecular reactions and  $\text{cm}^3 \text{mol}^{-1} \text{sec}^{-1}$  for bimolecular reactions.  $^1\text{X}$  = singlet;  $^3\text{X}$  = triplet.

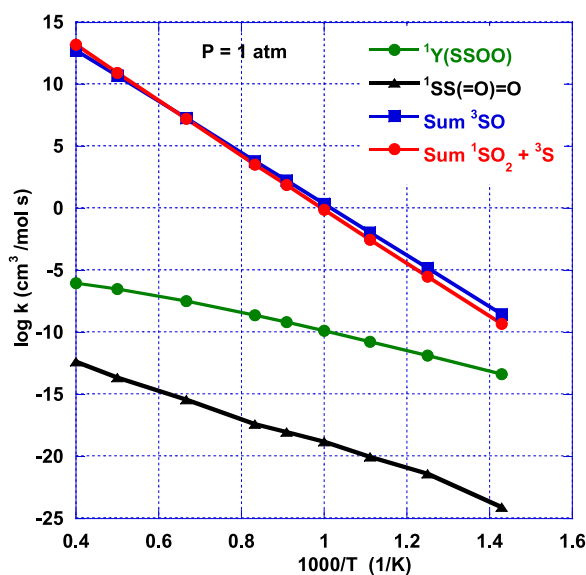
At low temperature, the overall rate coefficient for the formation of  $^1\text{SO}_2 + ^3\text{S}$  from the  $\text{cis-}^1\text{SSOO}$  is by orders of magnitude higher than the remaining ones. We note that the rate coefficient for the formation of the adduct  $\text{cis-}^1\text{SSOO}$  is lower by some orders of magnitude with decreasing tendency for the rate coefficients for the formation of  $^1\text{SS}(=\text{O})=\text{O}$  and the dissociation reaction channel to  $2^3\text{SO}$ . Due to the high barrier, the rate coefficients for the set of reactions leading to  $^1\text{SSO} + ^3\text{O}$  are very low.

As the temperature increases, the rate coefficients for the  $^1\text{SO}_2 + ^3\text{S}$  and  $^3\text{SO}$  formation reactions increase significantly, however, the rate coefficients of the channels to  $^1\text{SO}_2 + ^3\text{S}$  remain noticeably the highest. The rate coefficients for  $^1\text{SS}(=\text{O})=\text{O}$  formation reactions are also at comparable magnitude in this system, and increase with temperature as well. The rate coefficient for the dissociation of  $\text{cis-}^1\text{SSOO}$  to  $^1\text{SSO} + ^3\text{O}$  is, as expected, the lowest one due to the highest chemical activation energy of  $93.5 \text{ kcal}\cdot\text{mol}^{-1}$ , even as temperature increases. As the temperature increases, we note the stabilization of  $\text{cis-}^1\text{SSOO}$ , that may be explained by its fast conversion to  $\text{cis-}^1\text{OSSO}$  and  $^1\text{SS}(=\text{O})=\text{O}$ , both lying at a much lower energy level.

Figure 4 illustrates the rate coefficients for the formation of  $^1\text{Y}(\text{SSOO})$  and products from consecutive reactions of this intermediate at  $P = 1 \text{ atm}$ . At low temperature, the rate

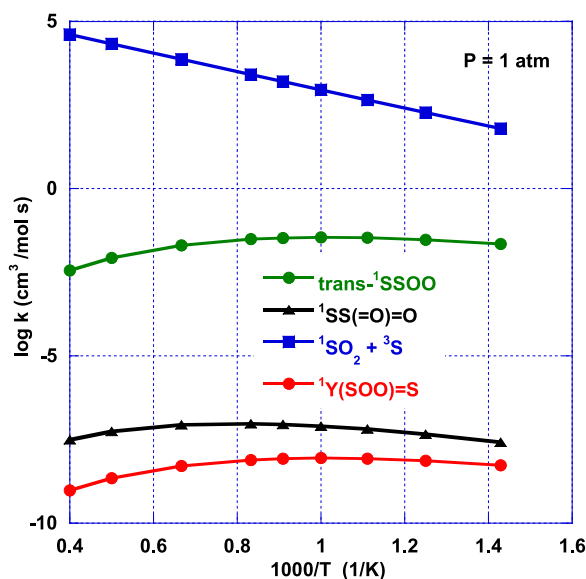


**Figure 3.** Calculated temperature-dependent rate coefficients for the formation of  $\text{cis-}^1\text{SSOO}$  from  $^3\text{S}_2 + ^3\text{O}_2$  and consecutive reactions at 1 atm.



**Figure 4.** Calculated temperature-dependent rate coefficients for the formation of  $^1\text{Y}(\text{SSOO})$  from  $^3\text{S}_2 + ^3\text{O}_2$  and consecutive reactions at  $P = 1$  atm.

coefficients for the set of reactions leading to  $^3\text{SO}$  as well as the  $^1\text{SO}_2 + ^3\text{S}$  are similar and the highest ones, both increasing as the temperature increases. It can be seen that the rate coefficients for the formation of the  $^1\text{Y}(\text{SSOO})$  adduct are lower. This can be explained as above by its facility to rearrange to the more energy-favorable  $\text{cis-}^1\text{OSSO}$  through only  $6.2 \text{ kcal}\cdot\text{mol}^{-1}$  energy barrier. The rate coefficient for the formation of  $^1\text{SS}(=\text{O})=\text{O}$  via



**Figure 5.** Calculated temperature-dependent rate coefficients for the formation of *trans*- ${}^1\text{SSOO}$  from  ${}^3\text{S}_2 + {}^3\text{O}_2$  and consecutive reactions at 1atm.

the sequential pathway is much lower due to two high barriers TS3-8 and TS3-9 for the isomerization reactions.

The pathway to the formation of the *trans*- ${}^1\text{SSOO}$  isomers as illustrated in Figure 2 consists first of the formation of  ${}^1\text{Y}(\text{SOO}) = \text{S}$  which releases an excess of energy by rearranging to a low energy  ${}^1\text{SS}(=\text{O}) = \text{O}$  isomer. This available energy allows the dissociation reaction of  ${}^1\text{SS}(=\text{O}) = \text{O}$  to  ${}^1\text{SO}_2 + {}^3\text{S}$ . Figure 5 exhibits that the reaction rate coefficient for the consecutive reaction of the *trans*- ${}^1\text{SSOO}$  isomer to  ${}^1\text{SO}_2 + {}^3\text{S}$  is by far the largest one. As the temperature increases, the rate coefficient of this reaction increases as well. The rate coefficient for the production of *trans*- ${}^1\text{SSOO}$  is lower and remains approximately constant with temperature. This is due to the direct isomerization reaction to  ${}^1\text{Y}(\text{SOO}) = \text{O}$ .  ${}^1\text{SS}(=\text{O}) = \text{O}$  and  ${}^1\text{Y}(\text{SOO}) = \text{S}$  are in this reaction path two intermediates, the rate coefficient for the formation of which is by orders of magnitude smaller.

## 4. Conclusions

This study investigates the thermochemistry of species and identifies the reactions paths resulting from the  ${}^3\text{S}_2 + {}^3\text{O}_2$  association. Enthalpies for a series of sulfur-oxygen compounds formed via the reactions in the  ${}^3\text{S}_2 + {}^3\text{O}_2$  system as well as transition state structures are calculated with the help of ab initio quantum chemistry calculations at CBS-QB3, G3B3, G4 and whenever possible at W1U levels. Reaction pathways describing the formation of the initial intermediates *cis*- ${}^1\text{SSOO}$ ,  ${}^1\text{Y}(\text{SSOO})$  and *trans*- ${}^1\text{SSOO}$  formed from  ${}^3\text{S}_2 + {}^3\text{O}_2$  as well as those describing successive reactions of the intermediate isomers are reported along with the rate coefficients of the reactions involved and identified in this system. Knowledge of the kinetic parameters and the products formed in this system as a

function of temperature and pressure is important for understanding and reaction modeling sulfur combustion. The rate coefficients of the reactions leading to  $^1\text{SO}_2 + ^3\text{S}$  and  $^3\text{SO}$  are by orders of magnitude the highest ones in the reaction system and increase steeply with increasing temperature. The results contribute to the development of detailed reaction mechanisms for sulfur combustion for use in energy generation.

## Note

1. In this article spin multiplicity of atoms and compounds are indicated whenever appropriate and necessary. If multiplicity is omitted, the notation comprises the predominantly existing electron spin configurations.

## Acknowledgements

The results presented in this study have been obtained within the framework of the SULPHURREAL Project.

## Disclosure statement

No potential conflict of interest was reported by the author(s).

## Funding

This project, SULPHURREAL, has received funding from the European Union's Horizon 2020 Research and Innovation Program [grant number 727540].

## References

- [1] Louie DK. Handbook of sulphuric acid manufacturing. Thornhill, Ontario: DKL Engineering, Inc.; 2005.
- [2] PEGASUS (H2020-LCE-2016-2017): Renewable power generation by solar particle receiver driven sulfur storage cycle. Horizon 2020. Competitive Low-Carbon Energy, 2016.
- [3] SULPHURREAL (Project 101115538): An innovative thermochemical cycle based on solid sulfur for integrated long-term storage of solar thermal, October 2023.
- [4] Zhang F, Kurjata M, Sebbar N, et al. Numerical study on flame stabilization and NO<sub>x</sub> formation in a novel burner system for sulfur combustion. *Energy Fuels*. 2022;36:4094–4106.
- [5] Marsden CJ, Smith BJ. An ab initio study of many isomers of S<sub>2</sub>O<sub>2</sub>. A combined theoretical and experimental analysis of the harmonic force field and molecular structure of cis-planar OSSO. *Chem Phys*. 1990;141:335–353.
- [6] Murakami Y, Onishi T, Kobayashi N, et al. High temperature reaction of S + SO<sub>2</sub> → SO + SO: implication of S<sub>2</sub>O<sub>2</sub> intermediate complex formation. *J Phys Chem A*. 2003;107:10996–11000.
- [7] Ramírez-Solís A, Jolibois F, Maron L. Born–Oppenheimer DFT molecular dynamics studies of S<sub>2</sub>O<sub>2</sub>: non-harmonic effects on the lowest energy isomers. *Chem Phys Lett*. 2011;510:21–26.
- [8] Frandsen BN, Wennberg PO, Kjaergaard HG. Identification of OSSO as a near-UV absorber in the Venusian atmosphere. *Geophys Res Lett*. 2016;43(11):146–155.
- [9] Frandsen BN, Farahani S, Vogt E, et al. Spectroscopy of OSSO and other sulfur compounds thought to be present in the Venus atmosphere. *J Phys Chem A*. 2020;124(35):7047–7059.
- [10] Herron JT, Huie RE. Rate constant at 298K for the reactions SO + SO + M → (SO)<sub>2</sub> + M and SO + (SO)<sub>2</sub> → SO<sub>2</sub> + S<sub>2</sub>O. *Chem Phys Lett*. 1980;76:322–324.
- [11] Hochlaf M, Linguerrri R, Cheraki M, et al. S<sub>2</sub>O<sub>2</sub>q + (q = 0, 1, and 2) molecular systems: characterization and atmospheric planetary implications. *J Phys Chem A*. 2021;125(9):1958–1971. doi:10.1021/acs.jpca.0c11407

- [12] Abumounshar M, Ibrahim S, Raj A. A detailed reaction mechanism for elemental sulphur combustion in the furnace of sulphuric acid plants. *Can J Chem Eng.* **2021**;99:2441–2451. doi:[10.1002/cjce.24185](https://doi.org/10.1002/cjce.24185)
- [13] Goodarzi M, Vahedpour M, Nazari F. Theoretical study on the atmospheric formation of cis and trans-OSSO complexes. *Chem Phys Lett.* **2010**;494:315–322.
- [14] Goodarzi M, Vahedpour M, Nazari F. Theoretical study on the mechanism of  $S_2 + O_2$  reaction. *Chem Phys Lett.* **2010**;497:1–6.
- [15] Frisch MJ, Trucks GW, Schlegel HB, et al. Gaussian 09, revision A02. Wallingford, CT: Gaussian, Inc.; **2016**.
- [16] Sebbar N, Bozzelli JW, Bockhorn H, et al. A thermochemical study on the primary oxidation of sulfur. *Combust Sci Technol.* **2019**;191(1):163–177.
- [17] Sebbar N, Bozzelli JW, Bockhorn H, et al. A thermochemical study of reactions occurring in the S-N-O system. *Proceeding of the Eleventh Mediterranean Combustion Symposium, Tenerife, Spain, 2019*; p. 16–20.
- [18] Montgomery JA, Frisch MJ, Ochterski JW, et al. A complete basis set model chemistry. VI. Use of density functional geometries and frequencies. *J Chem Phys.* **1999**;110:2822–2827.
- [19] Curtiss LA, Raghavachari K, Redfern PC, et al. Gaussian-3 (G3) theory for molecules containing first and second-row atoms. *J Chem Phys.* **1998**;109:7764–7776.
- [20] Baboul AG, Curtiss LA, Redfern PC, et al. Gaussian-3 theory using density functional geometries and zero-point energies. *J Chem Phys.* **1999**;110:7650–7657.
- [21] Curtiss LA, Redfern PC, Raghavachari K. Gaussian-4 theory. *J Chem Phys.* **2007**;126:0841081–08410812.
- [22] Martin JML, De Oliveira D. Towards standard methods for benchmark quality ab initio thermochemistry – W1 and W2 theory. *J Chem Phys.* **1999**;111:1843–1856.
- [23] Cox JD, Wagman DD, Medvedev VA. CODATA Key values for thermodynamics. New York: Hemisphere Publishing Corp.; **1984**.
- [24] Chase MW. NIST-JANAF thermochemical tables, fourth edition. *J Phys Chem Ref Data Monograph.* **1998**;9:1–1951.
- [25] Chang AY, Bozzelli JW, Dean AM. Kinetic analysis of complex chemical activation and unimolecular dissociation reactions using QRRK theory and the modified strong collision approximation. *Z Phys Chem.* **2000**;214:1533–1568. DOI: [10.1524/zpch.2000.214.11.1533](https://doi.org/10.1524/zpch.2000.214.11.1533).
- [26] Sheng C, Bozzelli JW, Dean AM, et al. Detailed kinetics and thermochemistry of  $C_2H_5 + O_2$ : reaction kinetics of the chemically-activated and stabilized  $CH_3CH_2OO\bullet$ . *Adduct J Phys Chem A.* **2002**;106:7276–7293.
- [27] Dean AM, Bozzelli JW, Ritter ER. CHEMACT: a computer code to estimate rate constants for chemically-activated reactions. *Combust Sci Technol.* **1991**;80:63–85.
- [28] Sheng C. Elementary, pressure dependent model for combustion of C1, C2 and nitrogen containing hydrocarbons: operation of a pilot scale incinerator and model comparison. PhD thesis, New Jersey Institute of Technology, Newark, USA, 2002.